Secondary Flows and Extra Heat Transfer Enhancement of Ribbed Surfaces With Jet Impingement

Z. Wang[+], Q. Zhang*, Y. Yan*, K. Liu[++], P. M. Ligrani[#]

[+] University of Michigan-Shanghai Jiao Tong University Joint Institute, Shanghai, P. R. China.
* School of Engineering and Mechanical Sciences, City University London, London, U.K.
[++] Siemens Industrial Turbomachinery Limited, Ruston House, Waterside South, Lincoln LN5 7FD, U.K.
[#] Propulsion Research Center, Department of Mechanical and Aerospace Engineering, University of Alabama in Huntsville, Huntsville, Alabama 35899 USA.

ABSTRACT

Previous experiments recognize that substantial heat transfer augmentation is achieved by adding ribbed turbulators after jet impingement with cross flow present. The present study investigates the fundamental working mechanism in a typical turbulent channel flow. Conjugate CFD simulations are employed for ribs, jet impingement, and their combinations. Flow characteristics and drawbacks for the individual and combined enhancement techniques are highlighted. New analysis on the coupled design arrangement reveals that the counter-rotating vortices generated by the jet flow can energize inter-rib recirculating vortices and promote spanwise convection. With an optimal design combination arrangement, extra heat transfer benefit is achieved beyond that associated with simple superposition of rib and jet impingement techniques. As such, the resulting thermal design approach is confirmed using published experimental data, and thus, is useful for surface heat transfer augmentation optimization in practice.

INTRODUCTION

In today's advanced gas turbine engine, many heat transfer enhancement technologies have been applied to the hot components, including ribs, pin fins, dimples, jet impingement, and film cooling, etc. [1-5]. To achieve the maximum cooling performance, combinations of different techniques are often applied to the components which experience extremely high thermal loadings, such as those associated with combustor liners and with high-pressure turbine blades and associated apparatus [2,4,6]. The general design philosophy is to promote the turbulent mixing and break the local thermal boundary layer. With many well-established conventional wisdoms associated with past heat transfer research, advancing the plateau in the existing cooling technology requires in-depth understanding of the detailed flow physics associated with combination designs.

Rib turbulators were found to be able to effectively reduce the thermal resistance by removing the near-wall viscous sub-layer. Rau *et al.* [7] experimentally studied the flow structures inside a ribbed straight channel and illustrated the existence of flow separation, reattachment as well as corner vortices. There have been many efforts on how to optimize the performance of ribs. Han [8] revealed that, the channel aspect ratio, the rib geometry and the flow Reynolds number dominated the heat transfer benefit of ribs. Han *et al.* [9] tested ribs with different angles of attack and concluded that placing ribs in an inclined angle (30-45 degree) against the cross flow could improve heat transfer and decrease pressure loss compared to the transverse arrangement. Han and Zhang [10] further introduced the broken V-shaped ribs and demonstrated superior heat transfer performance to other continuous ribs. Similar rib configurations were utilized by Ekkad and Han [11] as well. Such improvement was due to the introduction of secondary flow by the oblique ribs, as explained by Kim *et al.* [12]. Gao and Sundén [13] and Jia *et al.* [14] studied V-shaped ribs and associated the span-wise variation of heat transfer enhancement with the secondary flow motion, which essentially has been the main strategy to improve rib turbulator performance in the past years.

Jet impingement, as another widely used technique, is capable of boosting local heat transfer significantly by puncturing the boundary layer and promoting the turbulent mixing. The application of jet impingement requires vast pump power and high structural strength. In an early experiment, Gardon and Akfirat [15] studied the heat transfer enhancement of a circular impinging jet on a flat plate and highlighted the important role of turbulence in heat transfer augmentation. Apart from the stagnation point, they observed a secondary peak of heat transfer at two jet hole diameters away from the impingement center. The same flow pattern was verified by Viskanta [16]. Detailed flow features were investigated by Sakakibara *et al.* [17], and vortical structures were identified as the main source of extra turbulence generation. Angioletti *et al.* [18] further pointed out that the toroidal vortices were responsible for the maximum displacement of the heat energy.

Jet impingement is often implemented with the existence of cross flow. Bouchez and Goldstein [19] concluded that the addition of cross flow deflected the jet with the stagnation point moving downstream and the heat transfer enhancement was reduced compared to that with the absence of cross flow. Goldstein

and Behbahani [20] found the heat transfer benefit contributed by jet impingement was indeed weakened by cross flow at large jet-to-plate spacing (12 times of the jet hole diameter), but the opposite trend was observed when the spacing was narrowed (6 times of the hole diameter). Kim and Benson [21] numerically investigated the change in flow structures with the addition of cross flow and noticed the existence of a horseshoe vortex ahead of the jet and a pair of twin vortices in the jet wake, the generation of which was further explained by Chang *et al.* [22]. Nakade *et al.* [23] obtained extensive span-wise heat transfer augmentation by inducing a pair of longitudinal vortices through an oblique impinging jet flow.

The combination of jet impingement and rib turbulators were also well-studied. Gau and Lee [24] investigated a slot-jet impinging on a ribbed wall and found the surface roughness significantly altered the flow structure. Chang *et al.* [25] studied the effect of relative position of the jet to ribs and found that the best performance was achieved when the jet was oriented between ribs. The experiment conducted by Yan *et al.* [26] suggests that, when impinging on smooth walls, the existence of ribs might either strengthen or weaken the heat transfer depending on the arrangement of the ribs. Taslim and Fong [27] reported 30% higher heat transfer from the combination than impinging jet only.

The impingement and rib combination has often been applied with the presence of cross flow. This combination arrangement, as employed within past studies, varies significantly as different applications are considered. Most of these past studies address direct impingement onto ribbed surfaces. For example, Chang et al. [28] experimentally investigated the effect of various geometric parameters, such as relative position of the jet hole to the ribs, pitch-to-height ratio of the ribs and the jet-to-surface spacing, and the cross flow rate on flow structures. They reported the heat transfer enhancement was sensitive to these different conditions, and the introduction of ribs on a smooth surface could even weaken the heat transfer enhancement of an impinging jet when the pitch-to-height ratio of ribs was small. The effects of different rib configurations and blowing ratios were assessed by Rhee *et al.* [29]. They found that the ribs might not have beneficial contribution under low blowing ratios. In the heat transfer experiment by Wang et al. [30], an inclined jet impinged on a surface equipped with a single rib in a cross flow. Their results showed that

the presence of ribs expanded the stagnation point from a bell shape to a plateau shape and resulted in more uniform Nu distributions.

Different from the configuration from most studies, rib turbulators were added after jet impingement by Bailey *et al.* [4] in their experimental study for combustion liner cooling. Comparison was made against cases with either jet impingement or ribs employed individually. It was found that the presence of jet impingement promoted the heat transfer in the downstream ribbed region by 40% to 50%. This was reasoned by the authors as the increase in turbulence levels due to the jet impingement. The detailed flow physics behind this surprisingly high beneficial effect has not been explained.

Optimal thermal design will always be different for different operating conditions. More design space can only come from further understanding of the fundamental flow physics behind the many heat transfer experiments conducted over the past decades. Instead of optimizing a particular industrial design, this numerical study aims to look into the fundamental flow structure for ribs, jet impingement, and their coupling effect on conjugate heat transfer. The main motivation is consideration of qualitative and quantitative trends in flow physics, and understanding of associated thermal and flow variables and parameters for design optimization.

NOMENCLATURE

A	surface area of the bottom wall (m^2)
C_p	specific heat capacity of flow (J/kgK)
D_h	hydraulic diameter of the channel (m)
HTC	heat transfer coefficient (W/m^2K)
k	thermal conductivity of flow (W/mK)
$\dot{m}$	mass flow rate at channel exit (kg/sec)
Nu	Nusselt number
P	static pressure (Pa)
Q	heat flux at the bottom wall (W/m^2)
RANS	Reynolds-Averaged Navier-Stokes

s	distance from the leading edge of a rib (m)
S	distance between two adjacent ribs (m)
T	flow temperature (K)
TKE	normalized turbulent kinetic energy
u	flow velocity (m/sec)
w	width of the channel (m)
x	distance from the inlet (m)
X	length of the channel (m)
y	span-wise distance from one side (m)
ρ	flow density (kg/m^3)
θ	non-dimensional temperature
γ	flow vorticity (1/sec)
ζ	loss coefficient

Subscripts

0	flat channel
in	cross flow inlet
m	mean
w	wall

SUMMARY OF CASE STUDIES

A simplified channel flow was chosen in the present study. The geometry configuration is summarized first in this session.

The aspect ratio of the channel cross section is 2:1 and the channel length is 19 times of the height. Four cases have been studied:

Case 1 is a simple channel flow on a flat wall, which will be used as the baseline to assess the degree of heat transfer enhancement by the various techniques.

Case 2 includes rib turbulators on the bottom wall. There are total 14 ribs on the bottom of the channel with the block ratio of 1:10 and the height of the ribs equal to 7.5 percent of the channel hydraulic diameter. These squared ribs with pitch to height ratio of 10:1 are distributed evenly along the channel and oriented orthogonally to the cross flow. The first rib is four pitches from the entry.

Case 3 concerns jet impingement only. A single jet is introduced from the top of the channel only and the bottom of the channel remains flat and smooth. The impingement hole situates at four diameters downstream of the channel inlet and at the centre of span-wise with a diameter of a quarter of the channel width (half of the rib pitch).

Case 4 is the design of combining jet impingement and ribs. The arrangements of ribs and the jet impingement are the same as shown in Case 2 and Case 3.

COMPUTATIONAL METHOD

Fluid-solid conjugate analysis was conducted for all the four cases listed. The computational domain and the associated meshes for the combined ribs and jet impingement are presented in Figure 1. The overall domain consists of a rectangular flow channel with a thin solid layer placed at the bottom with the thickness of half of the rib height.

The commercial RANS CFD package ANSYS FLUENT 14.5 was applied to solve the three-dimensional, steady-state, turbulent hydro-thermal fields with the turbulence model chosen as K-Omega SST, which has been widely adopted to resolve adverse pressure gradients and flow separation.

Fully-developed velocity and temperature profiles were assigned as the inlet boundary condition. At the impingement hole, the velocity was specified as three times of the inlet mean velocity and the temperature is identical to that at the inlet. The overall mass flow rate at the exit of the channel remains the same in all the cases. Uniform heat flux of 2 kW/m^2 was supplied to the bottom of the solid wall. The top of the channel was regarded as a stationary adiabatic wall and both lateral sides were set with the periodic boundary condition.

The main purpose of adopting a conjugate model is to take into account the increase in the wetted area over the ribbed region and to reasonably compare local heat transfer enhancement among all cases

investigated. The Reynolds number based on the exit flow is 1×10^5. The solid material was aluminum, of which the thermal properties are listed in Figure 1 as well.

The commercial software Pointwise was employed to generate structured meshes for the present study. Mesh independence study was carried out by comparing the Nusselt number contours at the wall surface for three different density levels of grids. The Nusselt number was evaluated as $Nu = \frac{QD_h}{(T_w - T_m)k}$, where Q, D_h, T_w, T_m and k refer to surface heat flux, channel hydraulic diameter, wall temperature, local flow mean temperature and flow thermal conductivity respectively. Figure 2 presents the distribution of the relative difference in Nu between all three sets of grids with the one of 4.5 million grids as reference. The maximal local difference for 2.5 million grids goes beyond 3%, while that of 3.5 million grids is under 1%. Hence the 3.5 million grids were applied for all cases.

RESULTS AND DISCUSSION

Rib turbulator: pros and cons

Heat transfer enhancement by ribs is through not only enlarging the wetted surface area but also producing strong turbulence and destroying the boundary layer, hence altering the flow structures as detailed by Han *et. al.* [31]. Figure 3 is the results of Case 2. It presents the flow streamlines colored by velocity magnitude for one rib pitch and the Nu distribution along the rib surface.

For a typical flow between two parallel smooth walls, the boundary layers keep growing until reaching fully development profile. In contrast, the ribs extruding from the surface disturb the boundary layer repetitively and create periodic flow structures. As shown in Figure 3, flow separation happens at the front edge of the rib tip leading to a tiny separation region (zone 1). A substantially large after-rib recirculating vortex (zone 2) is established after the rib. Flow reattaches between two adjacent ribs and the local heat transfer is enhanced (zone 3). There is another corner vortex before the next rib (zone 4).

Compared to the baseline smooth wall case, heat transfer at the windward surface and the tip of ribs is significantly strengthened, due to the flow impingement and the regrowth of boundary layer. Meanwhile, the introduction of ribs also brings in extensive low-Nu regions locating between ribs.

Optimizing the thermal behavior over these regions or coupling other enhancement technique to enhance the performance in these regions has been the design focus in the past studies.

Jet impingement with cross flow

The application of jet impingement is to penetrate the cross flow and to impinge onto the wall surface with high velocity. As consequence, an extremely thin boundary layer in the impingement area is created and a pair of counter-rotating vortices downstream is induced.

Results of Case 3 are shown in Figure 4 and it illustrates streamlines of the jet flow colored by helicity and the non-dimensional temperature contour over the solid surface, with θ defined as $\theta = \frac{\dot{m}C_p(T-T_{in})}{QA}$. The two strands of intertwined streamlines show equivalent amount of helicity but with contrary signs, indicating they are rotating in opposite direction. And the region of the lowest temperature at the surface corresponds to the impingement area.

Figure 4 further presents the secondary flow vectors with a background of the turbulent kinetic energy contour over a cut-plane downstream of the impingement hole. The magnitude of the turbulent kinetic energy shown is normalized with respect to the mean value at the inlet. These velocity vectors indicate the transverse motion of near-wall fluids induced by the jet flow and demonstrate the redistribution of the boundary layer along the span-wise direction. The low-momentum fluids inside the boundary layer are driven to move laterally by the counter-rotating vortices, with part dragged off the surface and the rest stacked at two sides. Hence the boundary layer profile appears in a “U” shape. The turbulent kinetic energy is not uniformly spread as well. The turbulent mixing is strengthened significantly by the vortical structure and high-TKE fluids are rolled downwards closer to the area at center in accordance with the flow transverse movement.

All the above-mentioned factors promote heat transfer at the central region and result in the span-wise Nu distribution high in the central area as illustrated in Figure 5. This is supported by the fact that in Figure 4 the central zone is at a relatively lower temperature than both sides although the internal conduction lessens the transverse variation of the solid surface temperature. The magnitude of Nu at center is more

than two and half times of that without impingement, while the enhancement at sides is negligible. The average augmentation approximates to be twice of the case without jet impingement. Figure 5 also presents the stream-wise variation of the transversely averaged Nu over the entire computational domain. The peak of high Nu is found at the impingement region and then the level of elevated Nu declines continuously at the downstream. Such a trend is in conformity to the observation from Figure 4, where the flow helicity drops as travelling downstream and the surface temperature keeps rising after the impingement spot correspondingly.

Ribbed surface after jet impingement: flow structure

When ribs and jet impingement coupled together in a flow passage, their individual flow characteristics are still preserved. However, the interaction between jet impingement and the cavity flow between two adjacent ribs modifies the two individual flow patterns and leads to new secondary flow features as showed in Figures 6 and 7.

In Figure 6, the streamlines starting from the impingement hole colored by helicity demonstrate the existence of counter-rotating vortices. On two inter-rib cut-planes, the secondary flow velocity vectors are also superimposed with the contour of helicity. As indicated, the mainstream vortical structure above ribs energizes the inter-rib recirculating flow. Driven by the strong span-wise turbulent shear stress, two induced vortices with opposite rotating directions forms behind the rib. Such span-wise convection of the “dead” stream-wise recirculating fluids brings substantial augmentation in local turbulence, and more importantly, enhances the local heat transfer. Figure 7 presents a close-up view of the near wall turbulence kinetic energy and temperature gradient. Compared with the ribbed surface without impingement, the combination of rib and jet impingement has significant improvement.

Figure 8 compares the near-wall TKE distributions for all cases. For the channel with flat and smooth walls, the turbulent kinetic energy is at a very low level. The addition of jet impingement brings strong turbulent mixing inside vortices, creating a high-TKE footprint at the impingement spot and promoting the TKE at centre significantly. For the ribbed channel, the inter-rib recirculating vortex generates extra turbulence and slightly raises the TKE over the cavity floor. The windward surface of ribs blocks the near-

wall low-turbulence fluids and flow separation at the rib tips leads to the high TKE stripes. When both ribs and jet impingement are applied to the channel, a remarkable augmentation is achieved. The amount of turbulent mixing is even more than the superimposed value. The entire wall surface is immersed in flow with markedly higher TKE. The most striking growth occurs at the tip of ribs. The enhancement around the frontal edge of ribs is factually much higher than the simple summation of the benefit obtained from ribs and jet impingement individually. This is due to the combination of ribs' boundary layer removal and jet impingement's vortical structures, making the off-wall high-TKE fluids land onto the rib tips.

Ribbed surface after jet impingement: heat transfer

Figure 9 is the comparison of Nu distribution along a rib surface for Case 2 (ribbed enhancement only) and Case 4 (coupled enhancement of ribs with jet impingement). The introduction of additional jet impingement for the rib application succeeds in improving the heat transfer performance globally. The Nu around the dead corners is more than doubled. As discussed earlier, the benefit is a direct result of span-wise convection and TKE enhancement by involving jet impingement.

To evaluate the performance of ribs and jet impingement, the comparison of Nu distributions among all cases are made. Given the enlargement of the wetted area brought by ribs, Figure 10 shows the Nu contours at the flat bottom of the solid and Figure 11 plots the stream-wise variation of the span-wise averaged Nu. Since the solid is of high thermal conductivity and small thickness, the associated thermal resistance is negligible. So the Nu presented can reasonably reflect the flow convection. Meanwhile, the conduction inside the solid diminishes the difference of local heat transfer capabilities and smooths out the flow characteristics to some extent.

For the ribbed channel, arrayed stripe shadows can be observed in the Nu contour demonstrating the ribs' pump effect. The Nusselt number experiences a slight drop ahead of the ribbed region and then keeps growing steadily and stabilizing at 1.25. The application of jet impingement leaves a high-Nu footprint beneath the impingement hole and results in higher Nu at centre than at sides. The span-wise averaged Nu surges beyond 2 at the impingement region, but falls steadily after the peak with the value standing at 1.2 at the exit. In the case with the combination of ribs and jet impingement, due to the low Nu region ahead

of the first rib, the location of the maximum Nu region moves slightly downstream compared to the case with jet impingement only.

In Figure 11, the red dashed line represents the mathematical superposition of the augmentation from ribs and jet impingement individually. It is of interest to notice the red solid line exceeds the red dashed line throughout the entire region, although the gap between them narrows continuously and nearly vanishes at the end. The information conveyed is that additional heat transfer enhancement can be obtained by employing ribs and jet impingement at the same time. The extra benefit remains around 10% over the first twelve ribs in the present study.

The general trend observed in the present fundamental case study is also consistent with the previous work by Bailey *et al.* [4]. Their experimental data are replotted in Figure 12. The complicity of the channel geometry made it difficult to access accurate numerical results with details of the computational domain unknown. So only the published experimental data are presented without further CFD simulation. For this channel, there are five jet holes arranged in line at the top wall, creating the HTC oscillations at the impingement region. Heat transfer over the ribbed region of the case with jet impingement on ribs outperforms the summation of the enhancement from each technique individually. The addition augmentation even achieves above 50% at the region near the exit.

SUMMARY AND CONCLUSIONS

Substantial heat transfer augmentation is achieved by adding ribbed turbulators after jet impingement with cross flow. Within the present investigation, the fundamental working mechanism, behind this previous experimental finding, is numerically investigated. Employed for this purpose is fluid-solid conjugate analysis, conducted by using a commercial CFD tool.

Of particular importance are counter-rotating vortices induced by jet impingement, which induce spanwise convection for the inter-rib recirculating “dead” fluids. On the other hand, the rib turbulators also delay the heat transfer decay by jet impingement with cross flow. These complementary effects can be managed to produce extra heat transfer enhancement. The present results show that this management is

quantitatively more complex, than that which results from superposition of the effects of impingement array flows, with flow effects which result from wall-mounted rib turbulators.

The physical understanding from the present study can be further applied to the design optimization process in gas turbine heat transfer, particularly for components such as combustor liners and turbine blades subject to intensive heat loads. Although practical designs involve more complex geometries which may induce new flow features, the scenario utilized within the present investigation provides guidance and serves as a benchmark for further optimization.

REFERENCES

[1] D. Lorstad, LES and RNS Assessment of Rib Cooled Channel Related to SGT-800 Combustor Liner, ASME Paper No. GT2011-46415, TURBO EXPO 2011, ASME Turbine Technical Conference and Exposition, Vancouver, Canada, June 6-10, 2011.

[2] K. Liu, P. Martin, V. Sanderson, and P. Hubbard, Effect of Change in Fuel Compositions and Heating Value on Ignition and Performance for Siemens SGT-400 Dry Low Emission Combustion System, ASME Paper No. GT2013-94183, TURBO EXPO 2013, ASME Turbine Technical Conference and Exposition, San Antonio, Texas, USA, June 3-7, 2013.

[3] U. Ruedel, B. Trbojevic, U. Benz, M. Zajadatz, and K. Doebbeling, Development of an Annular Combustor Chamber, ASME Paper No. GT2013-95495, TURBO EXPO 2013, ASME Turbine Technical Conference and Exposition, San Antonio, Texas, USA, June 3-7, 2013.

[4] J. Bailey, J. Intile, T. Fric, A. Tolpadi, N. Nirmalan, and R. Bunker, 2002, “Experimental and Numerical Study of Heat Transfer in a Gas Turbine Combustor Liner,” ASME Paper No. GT2002-30183, TURBO EXPO 2002, ASME Turbine Technical Conference and Exposition, Amsterdam, The Netherlands, June 3-6, 2002.

[5] T. J. Jacobs, D. Underwood, and C. Lengsfeld, Optimization of Micro-Textured Surfaces for Turbine Vane Impingement Cooling, ASME Paper No. GT2013-95495, TURBO EXPO 2013, ASME Turbine Technical Conference and Exposition, San Antonio, Texas, USA, June 3-7, 2013.

[6] M. Miller, G. Natsui, M. Ricklick, J. Kapat, and R. Schilp, Heat Transfer In a Coupled Impingement-Effusion Cooling System, ASME Paper No. 2014-6416, TURBO EXPO 2014, ASME Turbine Technical Conference and Exposition, Dusseldorf, Germany, June 16-20, 2014.

[7] G. Rau, M. Cakan, D. Moeller, and T. Arts, The Effect of Periodic Ribs on the Local Aerodynamic and Heat Transfer Performance of a Straight Cooling Channel, ASME Transactions - Journal of Turbomachinery, vol. 120, no. 2, pp. 368-375, 1998.

[8] J. C. Han, Heat Transfer and Friction in Channels With Two Opposite Rib-Roughened Walls, ASME Transactions - Journal of Heat Transfer, vol. 106, no. 4, pp. 774-781, 1984.

[9] J. C. Han, J. Park, and C. Lei, "Heat Transfer Enhancement in Channels With Turbulence Promoters," ASME Transactions - Journal of Engineering for Gas Turbines and Power, vol. 107, no. 3, pp. 628-635, 1985.

[10] J. C. Han, and Y. Zhang, High Performance Heat Transfer Ducts With Parallel Broken and V-Shaped Broken Ribs," International Journal of Heat and Mass Transfer, vol. 35, no. 2, pp. 513-523, 1992.

[11] S. Ekkad, and J. C. Han, Detailed Heat Transfer Distribution in Two-Pass Channels With Rib Turbulators, International Journal of Heat and Mass Transfer, vol. 40, no. 11, pp. 2525-2537, 1997.

[12] R. Kiml, S. Mochizuki, and A. Murata, Effects of Rib Arrangements On Heat Transfer and Flow Behavior in a Rectangular Rib-Roughened Passage: Application to Cooling of Gas Turbine Blade Trailing Edge, ASME Transactions - Journal of Turbomachinery, vol. 123, no. 4, pp. 675-681, 2001.

[13] X. Gao, and B. Sundén, Heat Transfer Distribution In Rectangular Ducts With V-Shaped Ribs, Heat and Mass Transfer, vol. 37, no. 4-5, pp. 315-320, 2001.

[14] R. Jia, A. Saidi, and B. Sunden, Heat Transfer Enhancement in Square Ducts With V-Shaped Ribs," ASME Transactions - Journal of Turbomachinery, vol. 125, no. 4, pp. 788-791, 2003.

[15] R. Gardon, and J. Akfirat, The Role of Turbulence In Determining the Heat-Transfer Characteristics of Impinging Jets, International Journal of Heat and Mass Transfer, vol. 8, no. 10, pp. 1261-1272, 1965.

[16] R. Viskanta, Heat Transfer to Impinging Isothermal Gas and Flame Jets," Experimental Thermal and Fluid Science, vol. 6, no. 2, pp. 111-134, 1993.

[17] J. Sakakibara, K. Hishida, and M. Maeda, Vortex Structure and Heat Transfer in the Stagnation Region of An Impinging Plane Jet (Simultaneous Measurements of Velocity and Temperature Fields By Digital Particle Image Velocimetry and Laser-Induced Fluorescence), International Journal of Heat and Mass Transfer, vol. 40, no. 13, pp. 3163-3176, 1997.

[18] M. Angioletti, R. Di Tommaso, E. Nino, and G. Ruocco, Simultaneous Visualization of Flow Field and Evaluation of Local Heat Transfer By Transitional Impinging Jets, International Journal of Heat and Mass Transfer, vol. 46, no. 10, pp. 1703-1713, 2003.

[19] J. Bouchez, and R. J. Goldstein, Impingement Cooling From a Circular Jet In a Cross Flow, International Journal of Heat and Mass Transfer, vol. 18, no. 6, pp. 719-730, 1975.

[20] R. Goldstein, and A. Behbahani, Impingement of a Circular Jet With and Without Cross Flow, International Journal of Heat and Mass Transfer, vol. 25, no. 9, pp. 1377-1382, 1982.

[21] S. Kim, and T. Benson, Calculation of a Circular Jet In Crossflow With a Multiple-Time-Scale Turbulence Model, International Journal of Heat and Mass Transfer, vol. 35, no. 10, pp. 2357-2365, 1992.

[22] H. Chang, W. Chen, and T. Huang, Three-Dimensional Numerical Simulation of Impinging Jet Cooling With Initial Crossflow, ASME Paper 99-GT-256, TURBO EXPO 1999, ASME Turbine Technical Conference and Exposition, Indianapolis, Indiana, USA, June 7-10, 1999.

[23] K. Nakabe, K. Suzuki, K. Inaoka, A. Higashio, J. Acton, and W. Chen, Generation of Longitudinal Vortices In Internal Flows With An Inclined Impinging Jet and Enhancement of Target Plate Heat Transfer, International Journal of Heat and Fluid Flow, vol. 19, no. 5, pp. 573-581, 1998.

[24] C. Gau, and C. Lee, Impingement Cooling Flow Structure and Heat Transfer Along Rib-Roughened Walls, International Journal of Heat and Mass Transfer, vol. 35, no. 11, pp. 3009-3020, 1992.

[25] H. Chang, D. Zhang, and T. Huang, Impingement Heat Transfer From Rib Roughened Surface Within Arrays of Circular Jet: the Effect of the Relative Position of the Jet Hole to the Ribs, ASME Paper 97-GT-331, TURBO EXPO 1997, ASME Turbine Technical Conference and Exposition, Orlando, Florida, USA, June 2-5, 1997.

[26] W. Yan, H. Liu, C. Soong, and W. Yang, Experimental Study of Impinging Heat Transfer Along Rib-Roughened Walls By Using Transient Liquid Crystal Technique, International Journal of Heat and Mass Transfer, vol. 48, no. 12, pp. 2420-2428, 2005.

[27] M. Taslim, and M. Fong, Experimental and Numerical Crossover Jet Impingement in a Rib-Roughened Airfoil Trailing-Edge Cooling Channel, ASME Transactions - Journal of Turbomachinery, vol. 135, no. 5, pp. 051014-01 to 051014-09, 2013.

[28] H. Chang, J. Zhang, T. Huang, and D. Zhang, Flow Visualization of a Jet Impinging on a Ribbed Surface With Crossflow, Paper No. 96-TA-003, ASME 1996 Turbo Asia Conference, Jakarta, Indonesia, pp. V001T05A001, November 5–7, 1996.

[29] D. Rhee, Y. Nam, and H. Cho, Local Heat/Mass Transfer With Various Rib Arrangements In Impingement/Effusion Cooling System With Crossflow, ASME Transactions - Journal of Turbomachinery, vol. 126, no. 4, pp. 615-626, 2004.

[30] L. Wang, B. Sundén, A. Borg, and H. Abrahamsson, Control of Jet Impingement Heat Transfer in Crossflow by Using a Rib, International Journal of Heat and Mass Transfer, vol. 54, no. 19, pp. 4157-4166, 2011.

[31] J. C. Han, S. Dutta, and S. Ekkad, Gas Turbine Heat Transfer and Cooling Technology, Second Edition, CRC Press, Taylor and Francis Group, Boca Raton, Florida, USA, 2012.

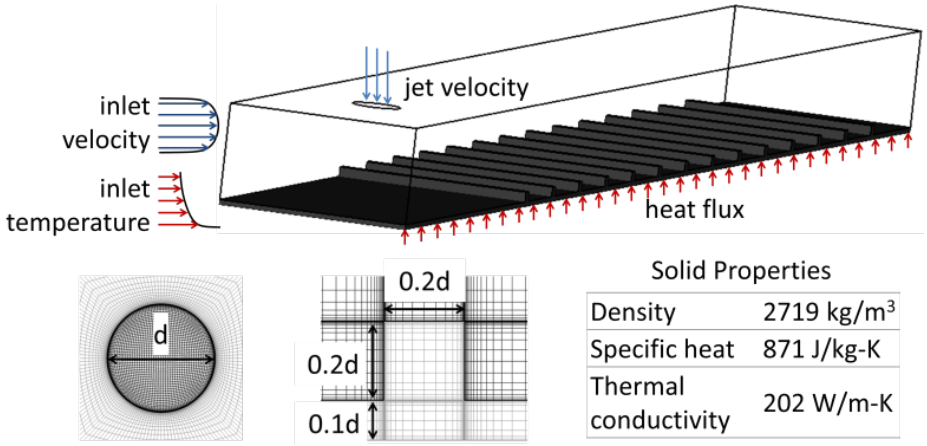

Figure 1. Computational domain and meshes.

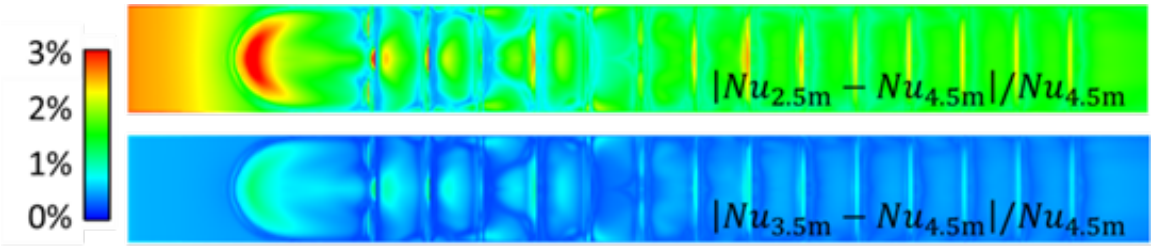

Figure 2. Grid independence study: Nusselt num ber variations for different grid density levels.

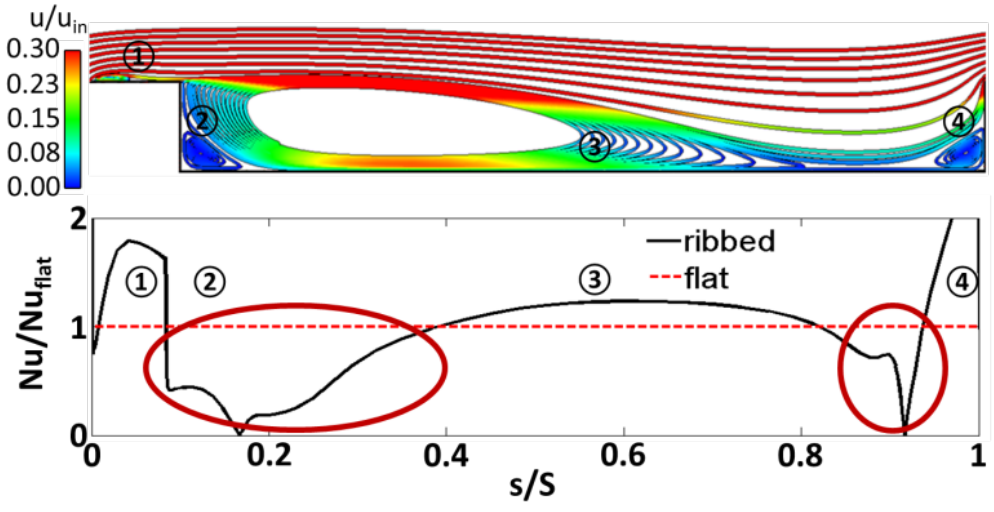

Figure 3. Flow structures in the ribbed channel: flow streamlines colored by velocity (top), and Nusselt number distribution on the rib surface (bottom).

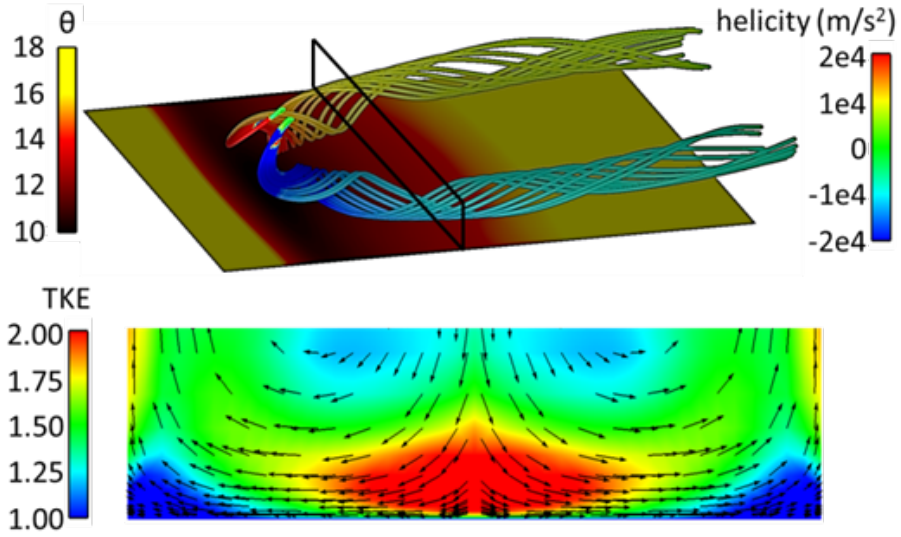

Figure 4. Flow structures in the flat channel with jet impingement: streamlines colored by helicity with temperature contour over the solid surface (top), and secondary flow vectors and turbulent kinetic energy contour over the cut-plane (bottom).

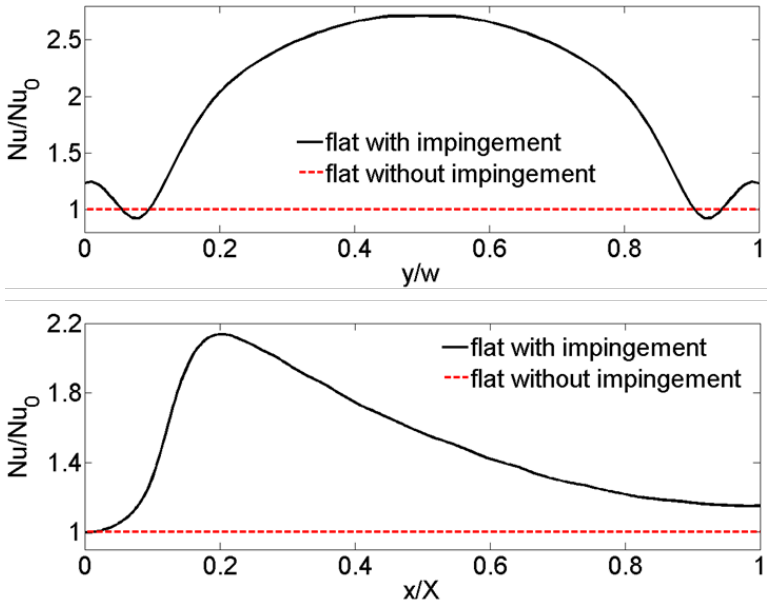

Figure 5. Nusselt number distribution in the flat channel with jet impingement along: the span-wise direction (top), and the stream-wise direction (bottom).

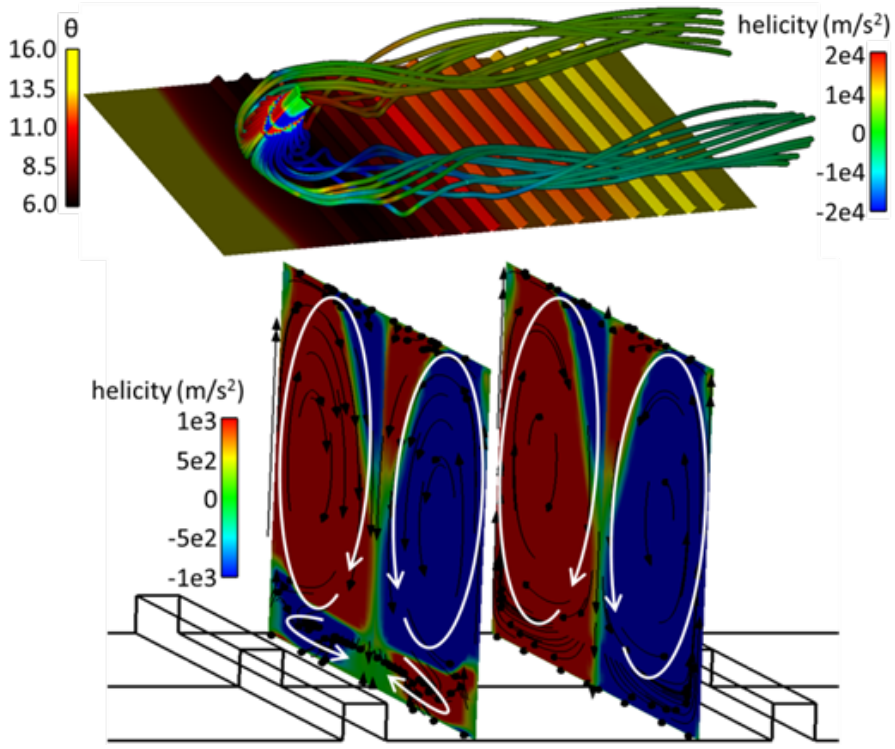

Figure 6. Flow structures in the channel with coupled ribs and jet impingement: (a) streamlines colored by helicity with temperature contour over the solid surface, (b) secondary flow vectors with helicity contours along two inter-rib cut-planes.

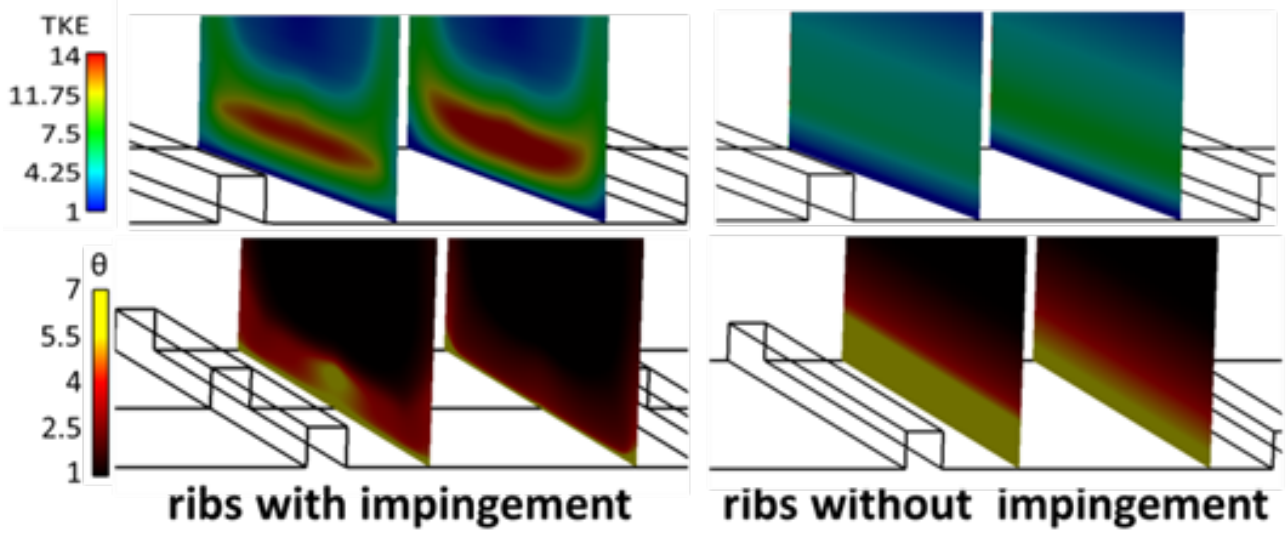

Figure 7. Near-wall TKE and temperature contours on the two cut-planes for: ribs with impingement (left), and ribs without impingement (right).

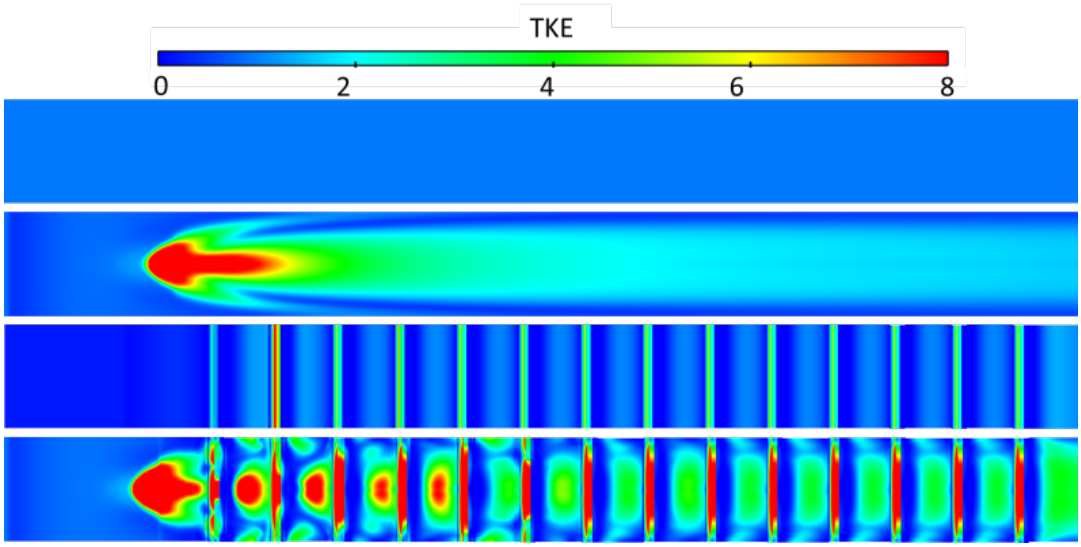

Figure 8. Near-wall TKE contours for all cases.

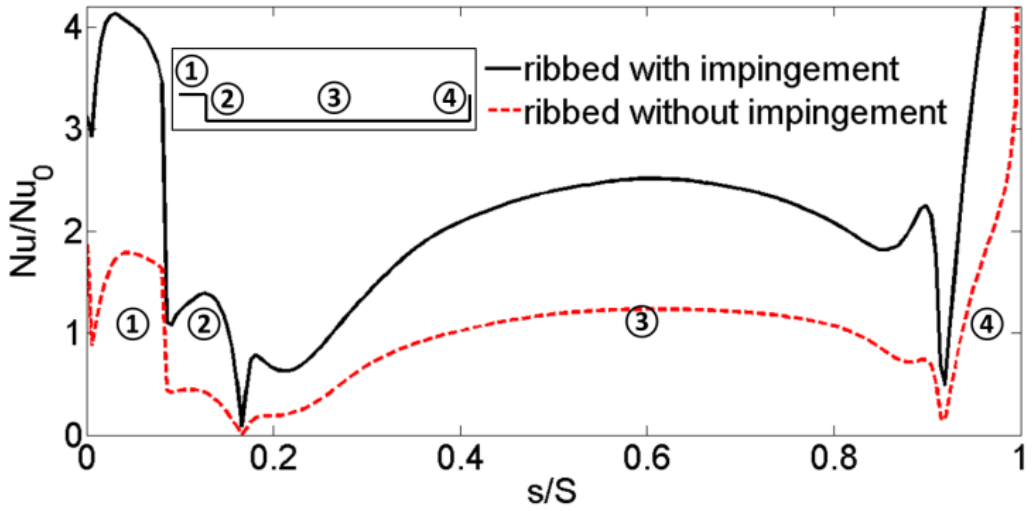

Figure 9. Comparison of Nusselt number distributions along a rib surface without jet impingement.

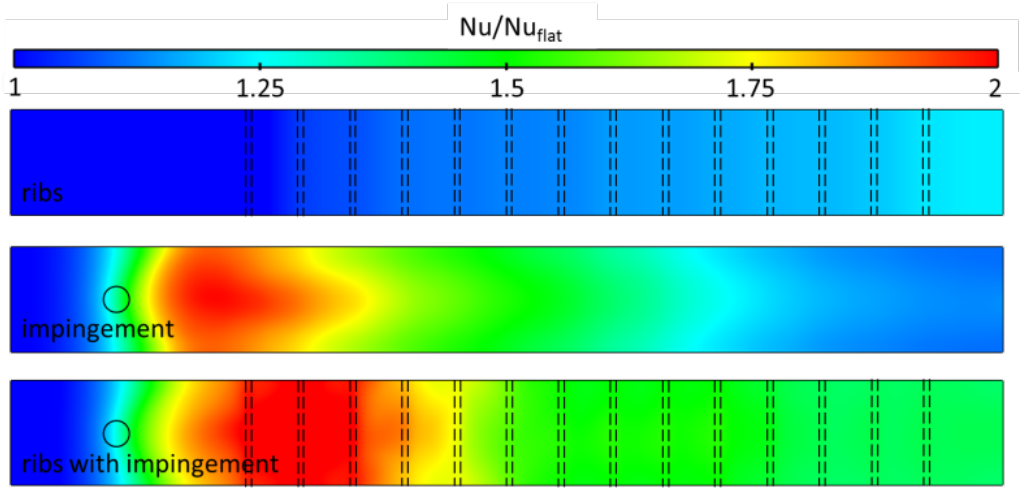

Figure 10. Normalized Nusselt number contours at the solid bottom.

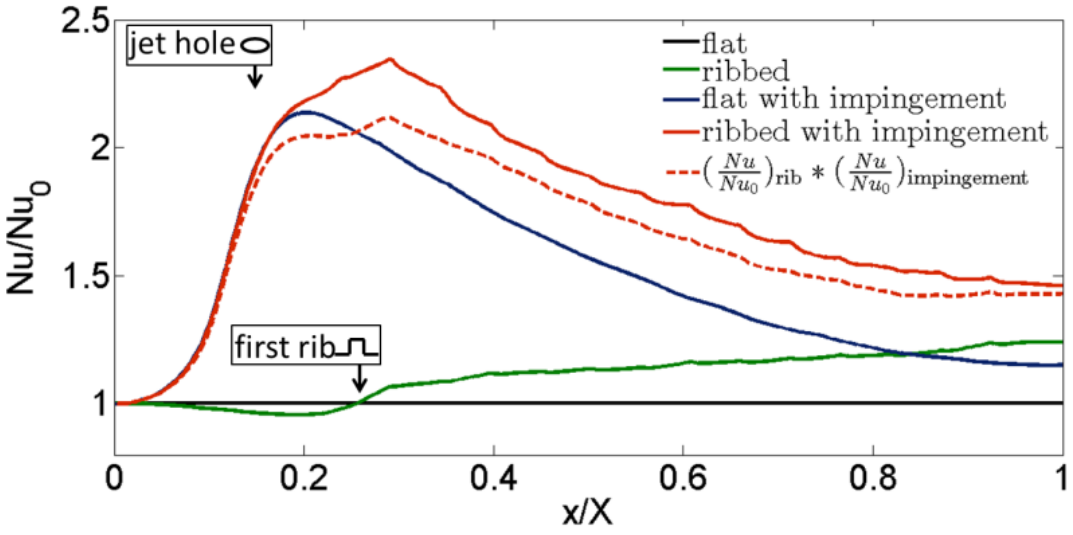

Figure 11. Spanwise averaged Nuseelt number values at the solid bottom.

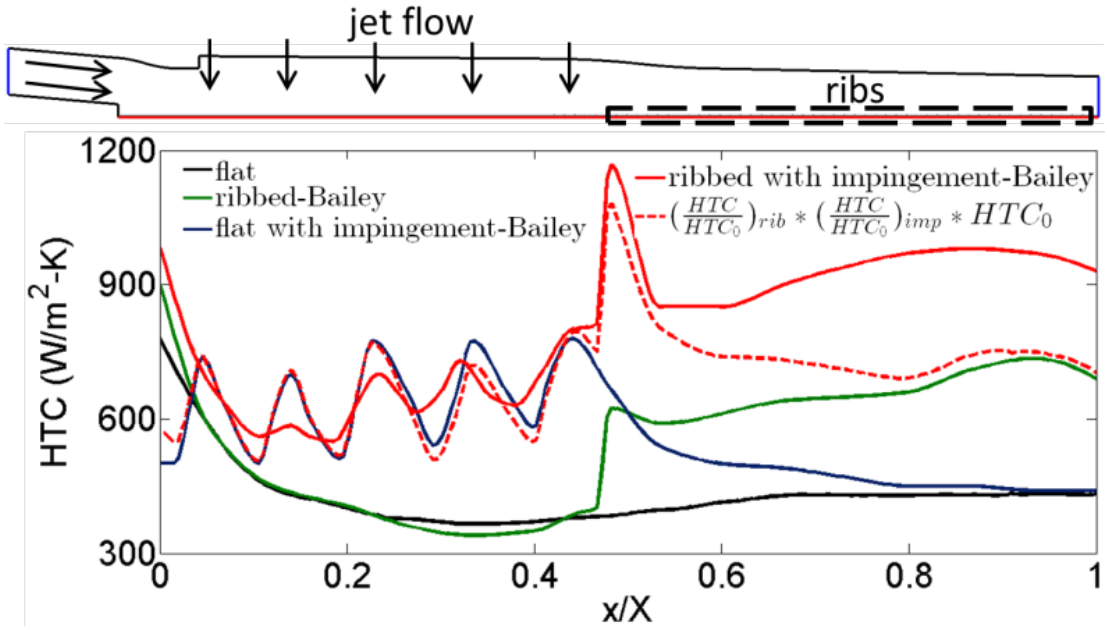

Figure 12. Comparisons of present results with experimental results from Bailey *et al.* [4].